



Planar microlenses applied to SPAD pixels

Lucie Dilhan, Jérôme Vaillant, Quentin Abadie, Alain Ostrovsky, Sébastien Verdet,
Pauline Calka, François Hemeret, L. Masarotto

► To cite this version:

Lucie Dilhan, Jérôme Vaillant, Quentin Abadie, Alain Ostrovsky, Sébastien Verdet, et al.. Planar microlenses applied to SPAD pixels. IISW 2021 - International Image Sensor Workshop, Jun 2021, Online, France. <10.60928/ygty-o9h9>. <hal-04617453>

HAL Id: hal-04617453

<https://hal.science/hal-04617453v1>

Submitted on 19 Jun 2024

HAL is a multi-disciplinary open access archive for the deposit and dissemination of scientific research documents, whether they are published or not. The documents may come from teaching and research institutions in France or abroad, or from public or private research centers.

L'archive ouverte pluridisciplinaire **HAL**, est destinée au dépôt et à la diffusion de documents scientifiques de niveau recherche, publiés ou non, émanant des établissements d'enseignement et de recherche français ou étrangers, des laboratoires publics ou privés.



HAL Authorization

Planar microlenses applied to SPAD pixels

L. Dilhan ^{1,2}, J. Vaillant ², Q. Abadie ², A. Ostrovsky ¹, S. Verdet ²,
P. Calka ², F. Hemeret ², L. Masarotto ²;

¹STMicroelectronics; 850 rue Jean Monnet, F-38920 Crolles; France

²Univ. Grenoble Alpes, CEA, LETI; F38000 Grenoble; France

Corresponding author: L. Dilhan: lucie.dilhan@st.com; +33 4 38 92 21 83.

Abstract – *Wafer level planar microlenses are designed to improve the sensitivity of SPAD arrays, based on rigorous optical simulations. State of the art refractive microlens solution and designed planar microlenses: FZP microlenses and metamicrolenses, are implemented on STMicroelectronics 40nm CMOS testchips (32×32 SPAD array).*

Optical gain compared to the reference microlens of 1.3 and 1.9 are shown for FZP and metamicrolenses, respectively in characterization and simulation.

Introduction

This paper follows the work of two papers [1, 2], for further inquiries on the background of the work, please refer to them.

Three types of microlenses are presented here: refractive microlenses, reference state of the art microlens for STMicroelectronics Single Photon Avalanche Diode (SPAD) pixels¹, and two types of planar microlenses: FZP microlenses and metamicrolenses, described in the next paragraphs. All three microlenses are embedded on top of SPAD pixels, processed either at STMicroelectronics or CEA-Leti clean-rooms.

The FZP microlens is a diffractive microlens based on X-ray lenses, we describe them as binary phase microlens focusing the incoming light at a chosen focal length. Such microlenses are simulated and processed on top of SPAD pixels, allowing to compare simulations to electro-optical characterizations in the first part of the article.

The second microlens is a metasurface encoded with a phase profile allowing the concentration of light at a given focal length. The metamicrolens is composed of sub-wavelength structurations, here pillars, of high-index material embedded in a low-index material.

Planar microlenses are compared to the reference refractive microlens, using Photon Detection Efficiency

(PDE²) as figure of merit. Due to the geometry of the SPAD array and the ability to design off-axis microlens with planar solutions, it is possible to increase the microlens footprint, hence the light collection area (see Fig.1). Simulation results of metamicrolenses embedded on SPAD pixels are shown in the second part of this article.

FZP microlenses results

Given the symmetry of the grouped photodiodes, we simulate only a quarter, hence in Fig.1, 2×2 SPAD pixels are outlined in orange, and off-axis planar microlenses are represented over them in blue, with their surface ranging from the surface of the photodiode pitch (written $\times 1$) to the maximum surface available between grouped photodiodes (written $\times 3.86$). The extension of the surface is presented in the patent we filed [4], and allows to increase the pitch of the microlens while not changing the photodiode pitch, thus gaining in PDE by absorbing light that was previously lost on the metal layers around photodiodes.

After performing simulations to select FZP microlenses designs with different surfaces, we implement them on top of SPAD pixels. We then characterize the different pixels at 940 nm to evaluate their performances compared to the reference refractive microlens. Their efficiency is given as the average PDE gain of all simulated or characterized pixels for one designed microlens, compared to the reference refractive microlens. We select a few designs from the simulations to be processed on top of SPAD pixels, and to be characterized.

We find a difference between simulation and characterization on Fig.2. This difference is explained by the source we use. In simulation, a normal incident plane wave at $940 \text{ nm} \pm 0 \text{ nm}$ is used as the source, whereas in characterization, a $940 \pm 5 \text{ nm}$ monochromatic source hits the wafer with an opening $f/2$ on the wafer.

¹As a reminder, this pixel functions with Front Side Illumination at 940 nm, the photodiodes are grouped 4×4 , allowing to increase their surface and leaving space between two consecutive groups.

²PDE is defined as the probability of an absorbed photon to generate an electron-hole pair and the probability of said pair to generate an avalanche inside the pixel, that will be recorded and read by the user [3].

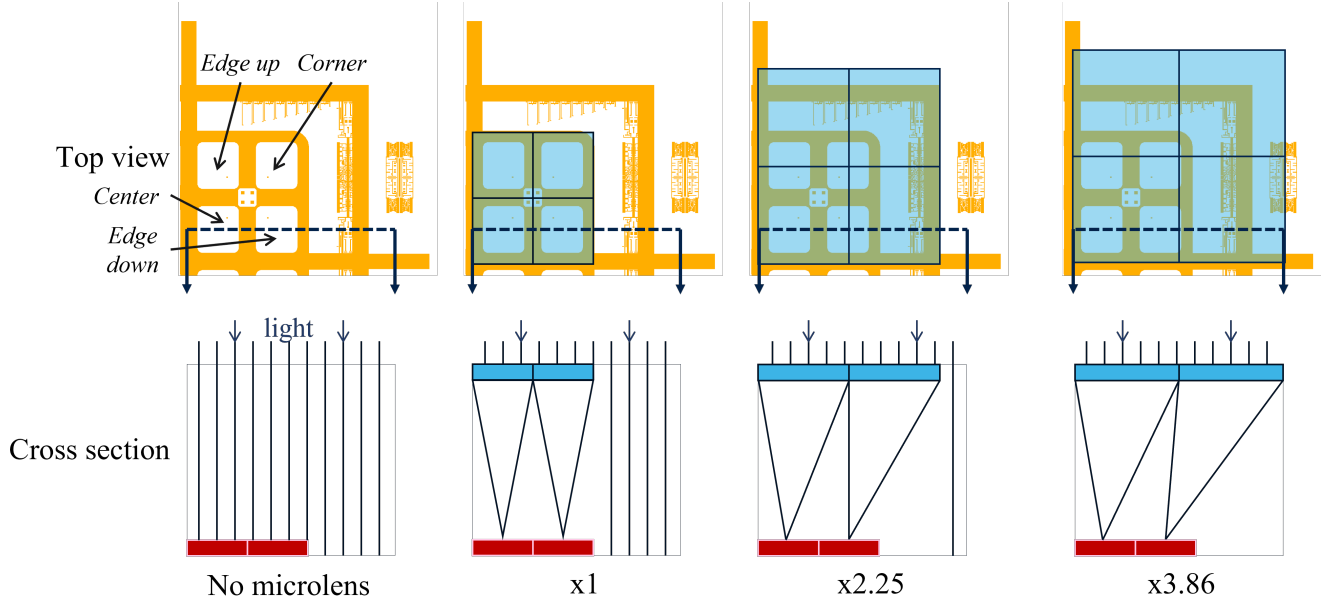


Figure 1: 2x2 SPAD pixels (orange) with and without planar microlenses (blue) with varying surfaces, focusing light in their associated photodiodes (red).

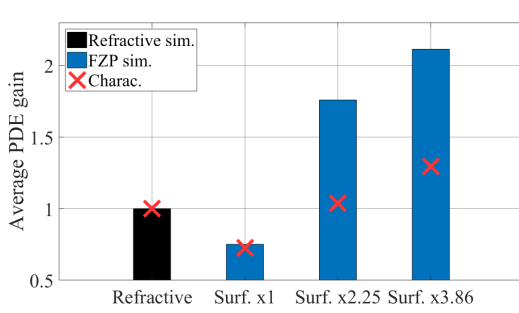


Figure 2: Refractive (black) and FZP (blue) microlenses simulated and characterized (red cross) average PDE gain over refractive microlens results, at 940 nm

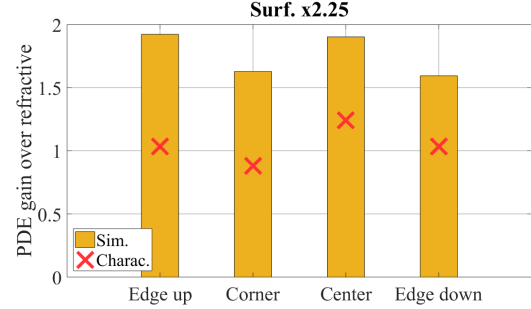


Figure 3: FZP PDE gain over reference microlens simulation results per pixel position inside the array.

To further investigate the difference between simulation and characterization, we look at PDE results obtained for each separated pixel, according to its position inside the array. The pixels are labeled *Edge up/down*, *Corner* and *Center*, as shown in Fig. 1 on the left. With a surface $\times 2.25$, we see in Fig. 3 that simulation and characterizations have the same trend according to the pixel position inside the array, thus validating the simulations and the process developed to integrate the FZP microlenses on SPAD pixels.

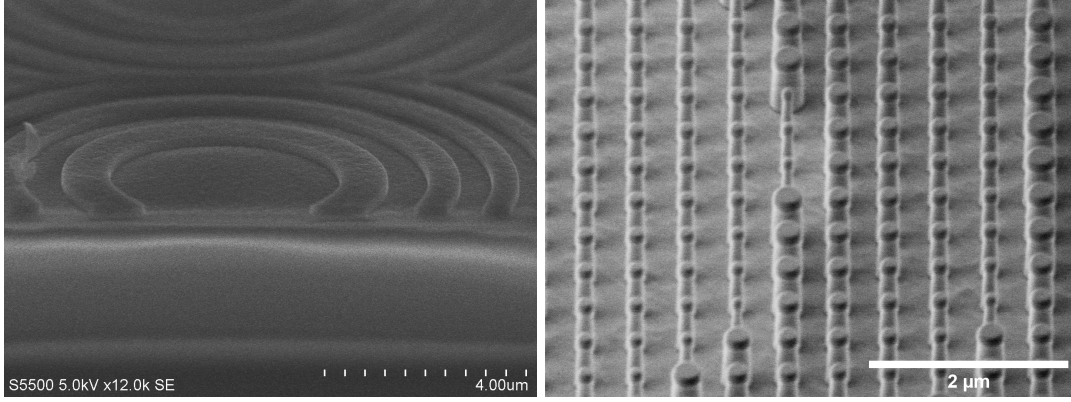
With Fig.4a we demonstrate our capability to process FZP microlenses on top of SPAD pixels, and with results presented in Fig.2 we demonstrate our capability to increase the average SPAD sensitivity, in characterization, up to a factor 1.3 with the largest FZP compared to the reference refractive microlenses.

To further increase PDE gain while using planar microlenses, we study metamicrosensors, to go from a binary microlens to a multi-phase microlenses.

Metamicrosensors study and results

Metamicrosensors creation method is described in Fig.7. The first step in metamicrosensors implementation is the simulation of unitary pillars, with their associated phase-shift and transmission. The pillars (with their parameters : diameter, height, period, lattice type, anti-reflective layer) are simulated using either RCWA or FDTD³ methods [5, 6]. Pillars varying only in diameter are gathered in libraries, that are sorted with crite-

³Rigorous Couple Wave Analysis or Finite Difference Time Domain



(a) FZP microlens tilted SEM cross-section view.

(b) Metamicrosensors tilted SEM view.

Figure 4: SEM views of FZP and metamicrosensors after lithography and etching steps during the process of fabrication.

ria such as overall transmission of the library or phase range of the gathered pillars. From the selected libraries, we can encode a metamicrosensors by arranging the pillars spatially either on a square or triangle lattice, the latter allowing pillars to be evenly spaced throughout the array, see Fig.5 [7], to be as close as possible to the ideal phase.



Figure 5: Square and triangle lattices, two possibilities to spatially place the pillars in a metamicrosensors.

Once the spatial arrangement is set, a file is generated and used to perform 3D FDTD simulations of metamicrosensors embedded on SPAD pixels, the same file is used to generate lithography masks.

Several metamicrosensors designs are simulated to obtain a microlens allowing a sensitivity gain on the reference refractive microlens. The varying parameters between the simulations are the lattice type and the microlens surface. All simulations are done with common pillar thickness, anti-reflective layer thickness and pillar period. Simulation results are gathered in Fig.6. We find a microlens with square lattice and surface $\times 3.86$ with an average PDE gain of 1.9 over the refractive microlens, this is to the best of our knowledge the highest optical gain demonstrated with planar microlenses on SPAD.

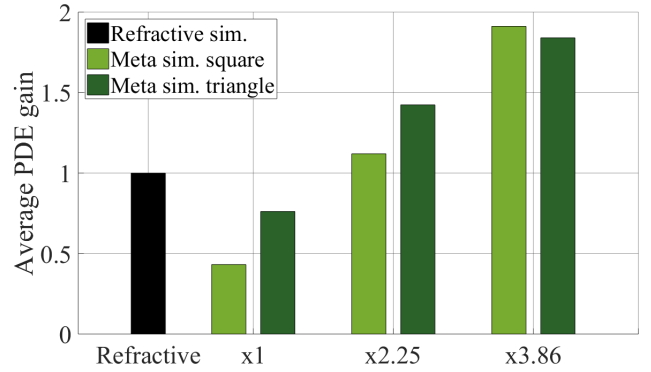


Figure 6: Refractive (black) and metamicrosensors (green) simulated average PDE gain over the reference microlens, at 940 nm. The surface of the metamicrosensors increases from left to right and the lattice is square (light green) or triangle (dark green).

Demonstrators with integrated metamicrosensors are currently under fabrication using a 193dry lithography tool. A tilted SEM view of the integrated pillars is shown in Fig.4b and Fig.8. The pillars are printed with the expected dimensions: diameter 100 nm and period 420 nm here.

Conclusion

We have demonstrated the capability to improve SPAD sensitivity by using different types of planar microlenses. We designed, simulated and processed Fresnel Zone Plate microlenses on STMicroelectronics 40nm CMOS testchips, and demonstrated an average 1.3 sensitivity gain on the reference refractive microlens in characterization. Metamicrosensors were designed and simulated and are currently being integrated on the same testchips.

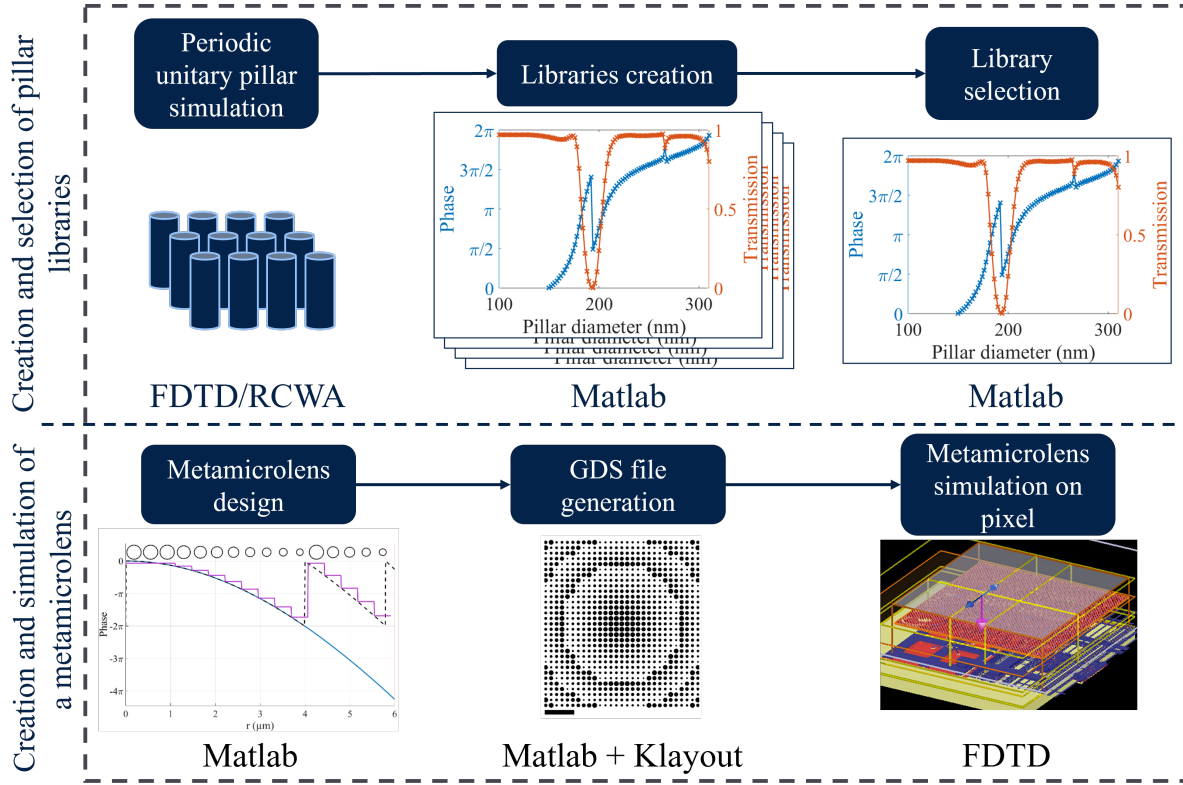


Figure 7: Metamicrolens creation method, from unitary pillar simulations to electro-magnetic wave propagation in full pixel stacks.

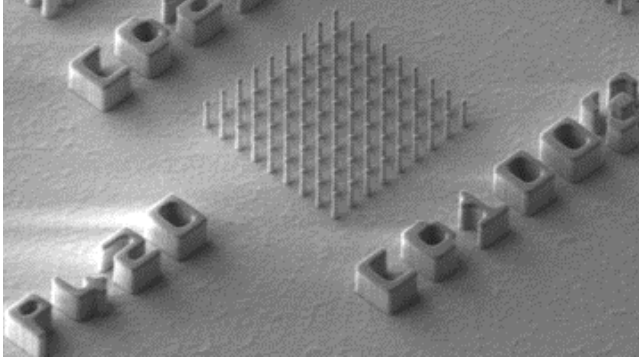


Figure 8: Printed pillars with period 420 nm and diameter 100 nm.

We have developed a patterning process that allows to reach the targeted pillar parameters. Average sensitivity gain of 1.9 over the refractive microlens is demonstrated in simulation.

Acknowledgements

We thank all the people that worked on the wafers in the cleanrooms both at STMicroelectronics and at the CEA Leti, particularly for the pillar process development.

References

- [1] J. Vaillant *et al.*, "SPAD array sensitivity improvement by diffractive microlens", In: *International Image Sensor Workshop (IISW)*, P28 (2019).
- [2] L. Dilhan *et al.*, "Planar microlenses for near infrared CMOS image sensors", In: *Electronic Imaging*, pp. 144.1-144.7 (2020).
- [3] S. Gnechi *et al.*, "Analysis of Photon Detection Efficiency and Dynamic Range in SPAD-Based Visible Light Receivers.", In: *Journal of Lightwave Technology*, vol. 34, no. 11, pp. 2774-2781 (2016).
- [4] L. Dilhan and J. Vaillant, "Image sensor", US20210111211 A1 2021-04-15 [US20210111211]-FR3102007 A1 2021-04-16 [FR3102007]-CN112736100 A 2021-04-30 [CN112736100]. (2019).
- [5] Mahmoud Elsayy *et al.*, "Global optimization of metasurface designs using statistical learning methods", In: *Scientific Reports* 9 (Nov. 2019).
- [6] Allen Taflov and S. Hagness. "Computational Electrodynamics: The Finite-Difference Time-Domain Method, 3rd edition", vol. 2062 (June 2005).
- [7] Branko Grünbaum and Geoffrey C. Shepard, "Tilings by Regular Polygons. Patterns in the plane from Kepler to the present, including recent results and unsolved problems.", In: *Mathematics magazine*, vol. 50, no. 5 (1977).